Catalysis Today 176 (2011) 149–153

Contents lists available at ScienceDirect

Catalysis Today

journal homepage: www.elsevier.com/locate/cattod

Hydroconversion of 1-methylnaphthalene over Pt/SBA-15 catalysts: Effect of SBA-15 chemical composition and method of binder incorporation

Jolanta R. Grzechowiak[a,*], Aleksandra Masalska[a], Karolina Jaroszewska[a], Karolina Sadowska[b]

[a] Faculty of Chemistry, Wrocław University of Technology, 7/9 Gdańska Str., 50-344 Wrocław, Poland
[b] Faculty of Chemistry, Jagiellonian University, 3 Ingardena Str., 30-060 Kraków, Poland

ARTICLE INFO

Article history:
Received 29 September 2010
Received in revised form
22 December 2010
Accepted 24 January 2011
Available online 5 March 2011

Keywords:
1-Methylnaphthalene hydroconversion
Pt catalysts
Binder
ZrSBA-15
AlSBA-15

ABSTRACT

The effect of the binder (boehmite, 20 wt.%) incorporation method and the chemical composition of the support (AlSBA-15, ZrSBA-15) on the physicochemical properties of Pt (2 wt.%) catalysts and on their activity in 1-methylnaphthalene hydroconversion was examined. The supports and catalysts were analyzed by N_2-sorption, XRD, ^{29}Si MAS NMR, ^{27}Al MAS NMR, XRF, H_2-chemisorption, Py-IR, NH_3-TPD, and TEM. When the binder was added to SBA-15 before impregnation with the Pt precursor, and when AlSBA-15 was used as a support, better Pt dispersion was obtained on the catalyst surface, which resulted in the improvement of the catalyst's hydrogenation properties.

1. Introduction

In the petroleum industry, the decrease in the content of aromatics is a crucial factor in the quality of the diesel oil obtained from crude oil refining processes. Dearomatization not only reduces the amount of particulates in the exhaust gases but also lowers the density of the fuel and increases the cetane number. When use is made of SBA-15 as support for hydrogenation catalysts, it is necessary to modify their acidity [1]. Since SBA-15 supports mainly occur in powder form, they have to be shaped (in industrial applications, it is common to use a binder). Studies into zeolites show that in metal/zeolite + binder systems activity, selectivity and stability depend not only on the type of the zeolite [2,3] and active metal used [4,5] but also on the quantity [6,7] and type of the binding agent [8,9].

In the literature only few publications can be traced regarding the formation of mesoporous materials [10–12]. Chandrasekar et al. [11], using bentonite as a binding agent to prepare SiSBA-15 extrudates, observed that the BET surface area (S_{BET}) of the powdered material (884 m^2/g) was reduced by 37% and by 60% upon formation with 2.2 wt.% of and 10.3 wt.%. of binder, respectively. When bentonite was used as a binder, the acidity of AlSBA-15 decreased due to the migration of alkaline earth metal ions from the binder to the acid sites of the mesoporous material [12]. Reduction in acidity upon bentonite incorporation was also observed during formation of the zeolite [4,7]. In contrast to natural aluminosilicates, alumina as binders enhanced the acidity of the zeolite-binder system in the majority of instances [5,7].

In the available literature no results have been reported regarding the effect of binder incorporation on the metal dispersion and hydrogenation activity of the catalysts where mesoporous materials were used as their supports. In keeping with the foregoing, it seemed to be of interest to study how the method used for binder incorporation (20 wt. % of boehmite) into Pt/SBA-15 influences surface chemistry and activity of Pt catalysts in 1-methyl-naphthalene conversion (1-MeN). Consideration was also given to the problem of how the isomorphous substitution Al or Zr for Si influences the properties of Pt/MeSBA-15 catalysts.

2. Experimental

2.1. Catalysts preparation

The mesoporous SiSBA-15 materials were prepared according to the method described by Kruk et al. [13]. AlSBA-15 and ZrSBA-15 (Si/M = 20) were synthesized by a direct hydrothermal method using $Al_2(SO_4)_3 \cdot 18H_2O$ and $Zr(SO_4)_2 \cdot H_2O$. Boehmite (Pural KR-1, Sasol GmBH; S_{BET} = 304 m^2/g, 0.54 mmol NH_3/g) was used as a binder. Two methods were used for binder incorporation. According to Method 1, SBA-15 was mixed with a solution of chloroplatinic

* Corresponding author. Tel.: +48 071 320 62 07; fax: +48 713206207.
E-mail address: Jolanta.Grzechowiak@pwr.wroc.pl (J.R. Grzechowiak).

0920-5861/$ – see front matter © 2011 Elsevier B.V. All rights reserved.
doi:10.1016/j.cattod.2011.01.027

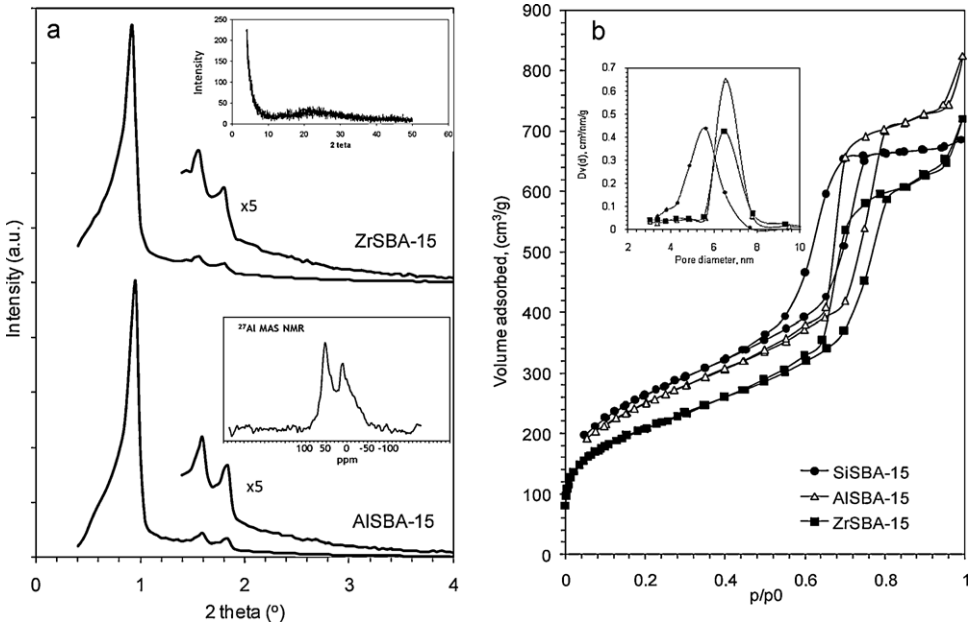

Fig. 1. Characteristics of mesoporous materials: (a) XRD patterns, ^{27}Al MAS NMR spectrum, and (b) N_2 adsorption–desorption isotherms.

acid (24 h), dried at 70 °C (3 h), and calcined; the final temperature being 450 °C (3 h). The extrudates were obtained using 20 wt.% of AlO(OH) and 3% nitric(V) acid (the catalyst is referred to as Pt/AlSBA-15(1)). According to Method 2, the mixture of boehmite and SBA-15 powders was impregnated with the Pt precursor, and after that the sample was dried (70 °C, 3 h) and calcined (450 °C, 3 h). The extrudates were obtained using 3% nitric(V) acid (the catalyst is referred to as Pt/MeSBA-15(2)). All extrudates were made subject to drying (110 °C, 12 h) and calcination (450 °C, 3 h).

2.2. Catalyst characterization

XRD and MAS NMR: X-ray patterns were obtained with Siemens 5005 diffractometer. ^{29}Si NMR and ^{27}Al MAS NMR spectra were recorded with an AC 200 Bruker spectrometer.

Surface morphology and porous structure: HRTEM images were obtained with a Philips CM-20 SuperTwin microscope. N_2 adsorption was measured at 77 K (Quantachrome, Autosorb-1C). Structural properties of mesoporous matrix were calculated as described elsewhere [14].

Acidity: Acidity was determined by adsorption of pyridine (Py-IR) and temperature-programmed desorption of ammonia (NH_3-TPD). Prior to acidity measurement via pyridine chemisorption, the samples were activated at 450 °C for 30 min. (10^{-5} mbar). IR spectra were recorded with a spectrometer Tensor 27 (Bruker). The A_{350}/A_{170} ratio where A_{170} is the intensity of the Py ion band upon evacuation at 170 °C and A_{350} is the intensity of the same band upon desorption at 350 °C was taken as a measure of the acid strength. When use was made of the NH_3-TPD method, acidity was evaluated in a through-flow system equipped with a thermal conductivity detector [15]. The sample was pre-treated in the stream of argon at 550 °C for 2 h and then cooled to 180 °C. After desorption of physically adsorbed ammonia, the sample was heated up to 550 °C at a rate of 10°/min.

Chemical analysis and dispersion: Pt content was determined by XRF (Canberra Packard, 1510) and Pt dispersion by H_2–O_2 titration (reduction at 500 °C for 5 h).

Catalytic experiments: Activity was tested during 1-MeN hydroconversion in a fixed-bed lab-scale microreactor at atmospheric pressure (240–350 °C, $W/F = 0.8$ g s/cm^3) and high pressure (280–380 °C, 5 MPa, H_2:CH = 500 Nm^3/m^3; WHSV = 2 h^{-1}, 10 vol.% 1-MeN in *n*-heptane).

3. Results and discussion

Small-angle XRD patterns (Fig. 1a) have revealed (1 0 0), (1 1 0), (2 0 0) reflections associated with the hexagonal space group p6mm [16]. Peak intensities are slightly better pronounced for AlSBA-15 than ZrSBA-15. Although the ionic radius of Zr^{4+} (86 pm) is noticeably larger than that of Si^{4+} (40 pm), in our work no increase in the value of the elementary cell parameter was observed (Table 1). The hypothetical variation of the cell parameters cannot be used as a proof to ascertain the incorporation of metal into the framework of mesoporous materials, as in the case of zeolites. The d_{100} values were reported to be very sensitive also to the degree of organization of the product [17]. No clear influence on the unit cell parameter due to the presence of Ti in the framework of MCM-41 has been demonstrated by Berlini et al. [18]. From the high-angle XRD pattern for ZrSBA-15 it is apparent that no ZrO_2 is present. This suggests that Zr has been well incorporated into the silica matrix, although the presence of small-sized Zr oxide species (<5 nm) outside the matrix, or of some Zr oxide species with poor crystallinity cannot be excluded. In the case of AlSBA-15 (the ionic radius of Al^{3+} amounted to 53 pm), the values of the elementary cell parameter were lower than for SiSBA-15. The incorporation of Al into the silica matrix is incomplete; ^{27}Al MAS NMR spectrum discloses the presence of extraframework aluminium (Fig. 1a). The presence of hexagonally packed mesostructures is confirmed by TEM (Fig. 2a). N_2 adsorption measurements also confirmed the presence of ordered mesoporous structures. All samples exhibit Type IV isotherms (N_2 adsorption sharply increases at p/p_0 of 0.7–0.75, Fig. 1b).

The condensation ratio of the mesoporous matrix was determined by the ^{29}Si MAS NMR method [19]. All spectra (not shown) exhibit broad, asymmetric signals, and were divided into three Gaussian lines with chemical shifts close to −91, −100 and −111 ppm for $Si(OSi)_2(O–X)_2$, $Si(OSi)_3(O–X)$ and $Si(OSi)_4$ units, where X is H, Al or Zr (Q_2, Q_3 and Q_4, respectively) (Table 1). The signals δ_{29Si} from Al or Zr containing species were overlapped with peaks from the silanol groups. Some researchers [20–23] also

Table 1
Characteristics of SBA-15 mesoporous materials.

Sample	29Si MAS NMR measurements			Structural properties of mesoporous matrix			Texture				Acidity by NH_3-TPD (μmol/g)
	Q_2[a] (%)	Q_3[a] (%)	Q_4[a] (%)	d_{100}[b] (nm)	a_0[c](nm)	w_t[d](nm)	S_{BET} (m^2/g)	Pore volume (cm^3/g)		d_{BJH}[e](nm)	
								V_T	V_{MIK}		
SiSBA-15	18.3	66.6	15.1	9.6	11.1	1.4	937	1.1	0.04	5.6	110
AlSBA-15	15.5	59.4	25.1	9.2	10.6	1.0	875	1.3	0.04	6.6	390
ZrSBA-15	11.0	17.8	71.2	9.6	11.1	1.3	720	1.1	0.02	6.5	450

[a] Surface % after deconvolution. $Q_2 = Si(OSi)_2(O–X)_2$, $Q_3 = Si(OSi)_3(O–X)$, $Q_4 = Si(SiO)_4$; where X stands for H, Al or Zr.
[b] Interplanar distance.
[c] Elementary cell parameter.
[d] Wall thickness.
[e] Average pore diameter (BJH method).

observed a shoulder at about −107 ppm attributed to Si(3Si,1Al) or Si(3Si,1Zr) species. In our work, the spectra exhibit no additional signal; the absence of that peak may be caused by the overlapping with the strong signal of the SiOH groups occurring at −100 ppm. For the ZrSBA-15 sample, we observed an additional shoulder at −95 ppm, which can be assigned to $(OSi)_2Si(OZr)(OH)$ [23]. This confirms that the zirconium atoms are incorporated into the SiO_2 matrix. The AlSBA-15 matrix mainly consists of $Si(OSi)_3(O–X)$ units (their proportion accounting for 59.4%). The spectrum of ZrSBA-15 has revealed a higher extent of Si lattice condensation, with a proportion of the $Si(SiO)_4$ groups exceeding 70%. In contrast to what was observed in the case of Zr, the thickness of the silica matrix wall (w_t) decreased after Al incorporation (Table 1). Textural parameter measurements show that the S_{BET} of SBA-15 decreased upon Al and Zr incorporation (Table 1). This should probably be attributed to a partial collapse of the hexagonal structure (observed in TEM Images – Fig. 2a). The incorporation of metals at the stage of synthesis increased the pore diameter by approx. 1 nm. NH_3-TPD results show that the acidity of ZrSBA-1 exceeds that of AlSBA-15 by about 60 μmol/g (Table 1).

The properties of the Pt catalysts differing in the method of binder incorporation and in the chemical composition of SBA-15 have been compiled in Table 2. Thus, when the binder was incorporated by Method 2, the catalyst exhibited a higher S_{BET} and a larger total pore volume (the comparison Pt/AlSBA-15(2) and Pt/AlSBA-15(1). The catalyst prepared with Method 2 also displayed a better Pt dispersion. The use of ZrSBA-15 for the preparation of the catalyst increased the Pt crystallite size (compared to AlSBA-15). The presence of larger Pt clusters on the surface of Pt/ZrSBA-15(2) is corroborated by TEM results (Fig. 2b). The poorer Pt dispersion in the Pt/ZrSBA-15(2) catalyst could be attributable to the Pt–Zr interaction [24].

Acidity measurements by Py-IR have revealed that the method of binder incorporation impacts on both the concentration and the strength of the acid sites (Table 3). When Method 2 was used (Pt/AlSBA-15(2)), the catalyst exhibited lower Lewis (L) acidity and higher Brønsted (B) acidity than when Method 1 was used (Pt/AlSBA-15(1)); the strength of B acid sites was weaker for catalyst Pt/AlSBA-15(2). An enhancement in B acidity and in the strength of B acid sites was observed upon the application of ZrSBA-15 (Pt/ZrSBA-15(2)) instead of AlSBA-15 (Pt/AlSBA-15(2)). A higher acidity of Pt/ZrSBA-15(2) was confirmed by NH_3-TPD (Table 3). NH_3-TPD profiles of both catalysts (not shown) indicate that ammonia is desorbed mainly over the range of 250–350 °C. The relative ratio of ammonia desorbed from Pt/ZrSBA-15(2) and Pt/AlSBA-15(2) at the temperatures at which the catalysts were tested (240, 280, 320 and 350 °C) is close to 1.75.

The activities of the Pt catalysts for 1-MeN hydroconversion at atmospheric pressure, and at 240–350 °C are shown in Table 4. The main products of 1-MeN hydroconversion are methyltetralins (MeTs). When the binder was incorporated by Method 2, the catalyst (Pt/AlSBA-15(2)) displayed a higher hydrogenating activity (higher 1-MeN conversion and methyldecalins (MeDs) yield) than when Method 1 was used (Pt/AlSBA-15(1)). The increased activ-

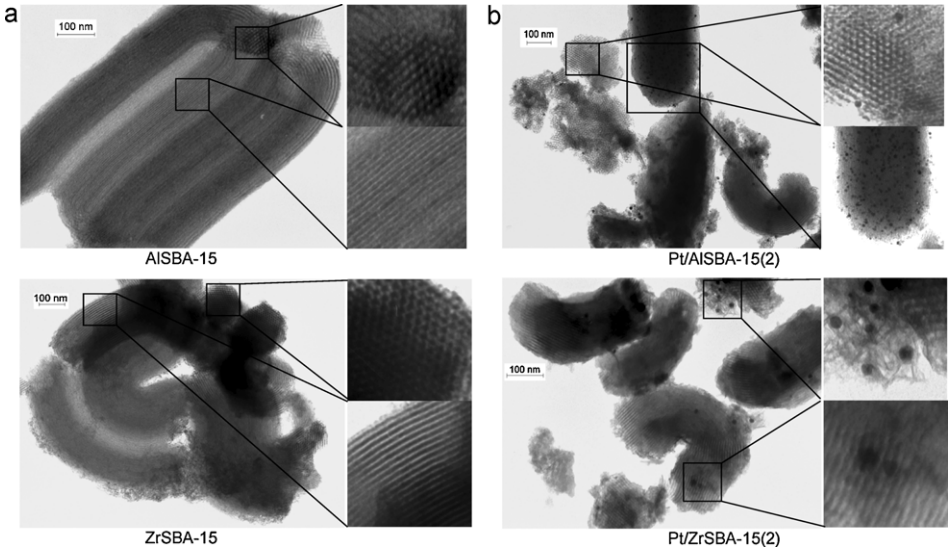

Fig. 2. TEM images of: (a) AlSBA-15 and ZrSBA-15 mesoporous materials, and (b) Pt/AlSBA-15(2) and Pt/ZrSBA-15(2) catalysts.

Table 2
Characteristics of Pt catalysts.

Catalyst	Pt[a] (wt.%)	D[b] (%)	S_{Met}[c] (m^2/g)	Crystallite size (nm)	S_{BET} (m^2/g)	Pore volume (cm^3/g)		d_{BJH}[d] (nm)
						V_T	V_{MIK}	
Pt/Al_2O_3	2.02	35.5	88.5	3.2	226	0.55	0.0	4.9
Pt/AlSBA-15(1)	1.86	16.1	40.1	7.0	425	0.58	0.02	4.9
Pt/AlSBA-15(2)	1.88	23.9	59.6	4.7	441	0.76	0.02	4.9
Pt/ZrSBA15(2)	1.78	16.3	40.6	6.9	435	0.68	0.0	5.6

[a] By XRF.
[b] Dispersion.
[c] Metal surface.
[d] Average pore diameter (BJH method).

Table 3
Acidity of Pt catalysts by Py-IR (effect of binder incorporation method and chemical composition).

Catalyst	APyH+ (μmol/g)			A_{350}/A_{170}	APyL (μmol/g)			A_{350}/A_{170}	NH_3-TPD (μmol/g)
	170 °C	250 °C	350 °C		170 °C	250 °C	350 °C		
Pt/Al_2O_3	0	0	0	–	248	185	132	0.53	510
Pt/AlSBA-15(1)	77	55	25	0.32	205	204	165	0.80	581
Pt/AlSBA-15(2)	98	72	26	0.27	154	151	129	0.84	520
Pt/ZrSBA-15(2)	124	85	46	0.37	220	217	192	0.87	640

Table 4
Activity of Pt catalysts in 1-MeN hydroconversion at 0.1 MPa (effect of binder incorporation method and SBA-15 chemical composition).

Catalyst	Reaction temperature (°C)	240	280	320	350
Pt/Al_2O_3	Conversion (%)	67.2	26.6	7.1	4.5
	MeDs yield (wt.%)	0.5	1.5	tr	tr
Pt/AlSBA-15 (1)	Conversion (%)	72.1	48.2	60.9	66.0
	MeDs yield (wt.%)	10.2	1.9	1.1	1.2
	cis-MeDs/*trans*-MeDs	0.2	–	–	–
Pt/AlSBA-15 (2)	Conversion (%)	78.2	63.4	68.1	69.6
	MeDs yield (wt.%)	15.8	2.8	1.8	1.7
	cis-MeDs/*trans*-MeDs	0.4	–	–	–
Pt/ZrSBA-15 (2)	Conversion (%)	63.0	36.9	32.3	46.5
	MeDs yield (wt.%)	10.5	1.3	0.5	tr
	cis-MeDs/*trans*-MeDs	0.4	–	–	–

ity of Pt/AlSBA-15(2) can be attributed not only to a better Pt dispersion but also to a higher B acidity. This means that 1-MeN hydrogenation occurs both on metal sites (conventional route) and acid sites (via hydrogen spillover). Method 2 provides a higher *cis*-MeDs/*trans*-MeDs ratio in the reaction products. According to the literature, in the hydrodecyclization reaction *cis*-decalin is more reactive than *trans*-decalin [24]. When the hydrodecyclization of aromatics occurs during their hydroconversion, this enhances the cetane number of the diesel oil fraction.

Concerning the effect of SBA-15 chemical composition on 1-MeN hydrogenation, it was found that even though Pt/ZrSBA-15(2) displayed a higher acidity, the MeDs yield over this catalyst was lower than over Pt/AlSBA-15(2). Hence, it can be postulated that because of a poorer Pt dispersion in Pt/ZrSBA-15(2), the yield of the metal sites involved in direct hydrogenation and the yield of the metal sites involved in hydrogen spillover were lower compared to Pt/AlSBA-15(2). All Pt catalysts supported on mesoporous materials show a higher activity compared to Pt/Al_2O_3 (Table 4). In sum, the use of Method 2 (binder combined with SBA-15 before impregnation with Pt precursor), as well as the use of AlSBA-15 as a support, seems to offer promise for the preparation of the catalysts for aromatics hydrogenation.

Table 5
Activity of Pt catalysts in 1-MeN hydroconversion at 5 MPa (effect of SBA-15 chemical composition).

Reaction temperature (°C)	Pt/AlSBA-15(2)				Pt/ZrSBA-15(2)			
	280	320	350	380	280	320	350	380
C_6–C_{10}	1.7	1.8	4.2	8.3	0.7	0.9	3.5	4.2
$\sum C_{11}$	65.7	76.0	75.6	69.1	47.7	56.3	67.1	51.9
MeDs	15.8	17.4	21.6	13.2	6.2	7.1	11.6	8.8
trans-MeDs	10.7	11.7	15.3	8.4	3.8	4.2	7.5	4.7
cis-MeDs	5.1	5.7	6.3	4.8	2.4	2.9	4.1	4.1
cis/*trans*-MeDs	0.5	0.5	0.4	0.6	0.6	0.7	0.6	0.9
ROP	0.2	0.4	1.7	3.4	0.3	0.5	1.0	2.9
MeTs	49.7	58.2	52.3	52.5	26.5	29.7	33.7	22.8
DMeIs	n.d.	n.d.	n.d.	n.d.	0.2	0.1	0.2	1.9
2-MeN	–	–	–		14.5	18.9	20.6	15.5
C balance (wt.%)	−3.0	−7.1	−12.0	−15.1	−4.9	−8.6	−15.4	−20.5
Conversion (wt.%)	70.4	84.9	91.8	92.5	53.3	65.8	86.0	76.6

The catalysts under study, which differed in the chemical composition of their supports (Pt/AlSBA-15(2), Pt/ZrSBA-15(2)), were tested for activity in 1-MeN hydroconversion also in high pressure experiments (Table 5). The reaction products were divided into C_{6-10} and C_{11} fractions. The mass balance between the feed and the liquid products was a measure of low-molecular-weight (LMW) products and carbonaceous deposits (CD). The C_{6-10} fraction contained mainly benzene, methylcyclohexane and toluene (low amounts of methylindens, decalins, and C_9-alkylbenzenes). In the C_{11} fraction detected were MeTs, MeDs, 2-methylnaphthalene (2-MeN), small amounts of dihydrodimethylindenes (DMeIs) and C_{11}-alkylbenzenes (ring opening product, ROP). Similarly to what was observed in the experiment at atmospheric pressure, Pt/AlSBA-15(2) exhibited a higher activity than did Pt/ZrSBA-15(2). The MeDs yield in the products obtained over Pt/AlSBA-15(2) was also higher. This indicates that the activity test at ambient pressure is useful for the preliminary assessment of the Pt catalyst's hydrogenation activity. Activity results at high pressure experiments show that the Pt/ZrSBA-15(2) catalyst displayed a higher activity in both cracking reaction (higher C balance) and isomerization reaction (formation of 2-MeN and DMeIs). This is attributable to the higher acidity of the Pt/ZrSBA-15 than Pt/AlSBA-15 catalyst. Even though in the reaction products obtained over Pt/ZrSBA-15(2) the *cis*-MeDs/*trans*-MeDs ratio was higher, the ROP yield was slightly lower, most probably because of the occurrence of a secondary cracking of the ROP.

4. Conclusions

The method of binder incorporation influences the activity and selectivity of Pt catalysts. When the binder (boehmite) is combined with AlSBA-15 before impregnation with the Pt precursor, the selectivity of Pt/AlSBA-15 to methyldecalins is higher, this can be attributed to the better Pt dispersion and higher Brønsted acidity (compared to the catalyst with the binder added to the Pt/AlSBA-15 powder).

The chemical composition of the support influences not only the acid properties of Pt catalysts but also Pt dispersion. Over the AlSBA-15 supported Pt catalyst, 1-methyl-naphthalene conversion and 1-methyldecalin yield were higher than over the ZrSBA-15 supported Pt catalyst, which can be attributed to a better Pt dispersion. The formation of dihydrodimethylindenes and 2-methylnaphthalene over the ZrSBA-15 supported Pt catalyst can be linked to the lower metal/acid ratio.

Acknowledgements

Financial support by the Ministry of Education and Science is gratefully acknowledged (1 T09B 07330).

References

[1] J. Wang, Q. Li, J. Yao, Appl. Catal. A 184 (1999) 181.
[2] F. Dorado, R. Romero, P. Cañizares, Appl. Catal. A 236 (2002) 235.
[3] A. de Lucas, J.L. Valverde, P. Sanchez, F. Dorado, M.J. Ramos, Appl. Catal. A 282 (2005) 15.
[4] A. de Lucas, M.J. Ramos, F. Dorado, P. Sanchez, J.L. Valverde, Appl. Catal. A 289 (2005) 205.
[5] P. Sanchez, F. Dorado, M.J. Ramos, R. Romero, V. Jimenez, J.L. Valverde, Appl. Catal. A 314 (2006) 248.
[6] Y. Zhang, Y. Zhou, A. Qiu, Y. Wang, Y. Xu, P. Wu, Ind. Eng. Chem. Res. 45 (2006) 2213.
[7] M.W. Kasture, P.S. Niphadkar, V.V. Bokade, P.N. Joshi, Catal. Commun. 8 (2007) 1003.
[8] F. Dorado, R. Romero, P. Cañizares, Ind. Eng. Chem. Res. 40 (2001) 3428.
[9] V.R. Choudhary, P. Devadas, A.K. Kinage, M. Guisnet, Appl. Catal. A 162 (1997) 223.
[10] M. Hartmann, S. Kuntz, G. Chandrasekar, V. Murugesan, Stud. Surf. Sci. Catal. 165 (2007) 181.
[11] G. Chandrasekar, M. Hartmann, V. Murugesan, J. Porous Mater. 16 (2009) 175.
[12] G. Chandrasekar, M. Hartmann, M. Palanichamy, V. Murugesan, Catal. Commun. 8 (2007) 457.
[13] M. Kruk, M. Jaroniec, S.H. Joo, R. Ryoo, J. Phys. Chem. B 107 (2003) 2205.
[14] L.A. Rios, P. Weckes, H. Schuster, W.F. Hoelderich, J. Catal. 232 (2005) 19.
[15] A. Masalska, Appl. Catal. A 294 (2005) 260.
[16] H. Huang, C. Yang, H. Zhang, M. Liu, Micropor. Mesopor. Mater. 111 (2008) 254.
[17] T. Blasco, A. Corma, M.T. Navarro, J.P. Pariente, J. Catal. 156 (1995) 65.
[18] Ch. Berlini, M. Guidotti, G. Moretti, R. Psaro, N. Ravasio, Catal. Today 60 (2000) 219.
[19] M. Hunger, U. Schenk, M. Breuninger, R. Gläser, J. Weitkamp, Micropor. Mesopor. Mater. 27 (1999) 261.
[20] G.V. Shanbhag, S.M. Kumbar, S.B. Halliqudi, J. Mol. Catal. A: Chem. 284 (2008) 16.
[21] A. Matsumoto, H. Chen, K. Tsutsumi, M. Grün, K. Unger, Micropor. Mesopor. Mater. 32 (1999) 55.
[22] G.V. Shanbhag, T. Joseph, S.B. Halligudi, J. Catal. 250 (2007) 274.
[23] J.H. Choy, J.B. Yoon, H. Jung, J.H. Park, J. Porous Mater. 11 (2004) 123.
[24] Ch.K. Mouli, V. Sundaramurthy, A.K. Dalai, Z. Ring, Appl. Catal. A 321 (2007) 17.